ORIGINAL ARTICLE

Staphylococcus aureus impairs cutaneous wound healing by activating the expression of a gap junction protein, connexin-43 in keratinocytes

Wei Xu[1] · Elodi Dielubanza[2] · Amanda Maisel[2] · Kai Leung[3] · Thomas Mustoe[2] · Seok Hong[2] · Robert Galiano[2]

Abstract

Chronic wounds have been considered as major medical problems that may result in expensive healthcare. One of the common causes of chronic wounds is bacterial contamination that leads to persistent inflammation and unbalanced host cell immune responses. Among the bacterial strains that have been identified from chronic wounds, *Staphylococcus aureus* is the most common strain. We previously observed that *S. aureus* impaired mouse cutaneous wound healing by delaying re-epithelialization. Here, we investigated the mechanism of delayed re-epithelialization caused by *S. aureus* infection. With the presence of *S. aureus* exudate, the migration of in vitro cultured human keratinocytes was significantly inhibited and connexin-43 (Cx43) was upregulated. Inhibition of keratinocyte migration by *S. aureus* exudate disappeared in keratinocytes where the expression of Cx43 knocked down. Protein kinase phosphorylation array showed that phosphorylation of Akt-S473 was upregulated by *S. aureus* exudate. In vivo study of Cx43 in *S. aureus*-infected murine splinted cutaneous wound model showed upregulation of Cx43 in the migrating epithelial edge by *S. aureus* infection. Treatment with a PI3K/Akt inhibitor reduced Cx43 expression and overcame the wound closure impairment by *S. aureus* infection in the mouse model. This may contribute to the development of treatment to bacterium-infected wounds.

Keywords Skin wound repair · *Staphylococcus aureus* · Connexin 43 · Re-epithelialization

Introduction

Unlike most regular wounds, chronic wounds are a common and costly clinical problem due to their unpredictable amount of healing time. 1–2% of Americans are estimated to develop chronic wounds within their lifetime and related annual healthcare spending is upwards of $32 billion [1]. Chronic wounds were long recognized to be caused by several chronic diseases, such as diabetes, vascular disease, and chronic kidney disease. Over the last decade, wound-healing research has confirmed that this wound phenotype also depends on multiple external factors.

Bacterial infections have been shown to be ubiquitous in these wounds and mounting literature suggests that they are prime actors in the creation and maintenance of chronic wounds [2–5]. Like other known bacterial infection-related diseases, chronic wounds are persistent, unresponsive to antimicrobial therapy and resistant to host immune eradication.

Among a number of bacteria that can colonize chronic wounds, *Staphylococcus aureus*, *Pseudomonas aeruginosa*, *β-hemolytic streptococcus,* and anaerobes are the most

✉ Wei Xu
wei.xu@tamucc.edu

✉ Seok Hong
seok-hong@northwestern.edu

✉ Robert Galiano
rgaliano@nm.org

1 Department of Life Sciences, College of Science and Engineering, Texas A&M University-Corpus Christi, Corpus Christi, TX 78412, USA

2 Laboratory for Wound Repair and Regenerative Surgery, Department of Surgery, Northwestern University Feinberg School of Medicine, Chicago, IL 60611, USA

3 Division of Combat Wound Repair, US Army Institute of Surgical Research, JB Fort Sam Houston, San Antonio, TX 78234, USA

common causes of delayed healing [6]. *S. aureus* is the predominant strain of these chronic wound-associated bacteria [7]. As a Gram-positive coccus, *S. aureus* is known to colonize the wound beds with the assistance of secreted proteases and toxins [8]. However, a few authors have explored the mechanism of the impairment caused by the presence of bacterial infection.

Most typical chronic wounds have an essential feature: lacking the ability in epidermis restoration, which is primarily directed by the migration of keratinocytes. Introducing bacterial infections in the wound disrupts the balance in re-epithelialization and increases the complexity of the factors determining the migration of keratinocytes. Several studies suggest that colonization of bacteria in the wound bed results in excessive inflammation producing a great amount of pro-inflammatory factors [9, 10]. However, fully colonized bacteria may produce an extracellular polymeric substance (EPS) to protect themselves from being eliminated by immune cells [4] which consequently leads to prolonged bacterial clearance resulting in a non-healing chronic wound.

The migration of keratinocytes in epidermal wounds was described as the collective movement of a group of cells in the in vivo [11–13] and in vitro models [14]. During cell migration, a number of cell–cell junction proteins demonstrated a similar expression pattern including cadherin [13], occludin [12], and connexins [11]. Earlier studies suggested that connexins are involved in keratinocyte migration in wounded sites [15].

Connexins (also known as gap junction proteins, GJPs) are a large family of transmembrane proteins that have both channel dependent and independent functions and play a role in cell growth, differentiation, and signaling. A wide variety of connexins have been identified from cells in different tissues including skin. The roles of these various types of connexins in the skin are not completely clear, but the importance of these connexins has been recognized, since many of them are associated with skin diseases, such as hystrix-like ichthyosis with deafness, keratitis-ichthyosis-deafness syndrome, Vohwinkel syndrome, and erythrokeratodermia variabilis [16–19].

Among all the connexins detected in skin, Cx43 is the subtype most prominently expressed in epidermis and has been shown to impact keratinocyte proliferation, migration, and differentiation [20]. In normal wound healing, Cx43 is downregulated at the skin margins early in the process markedly reducing the number of gap junctions and enabling cell migration [20–22]. Knockdown of Cx43 expression by gene knockout or Cx43 antisense oligonucleotide was shown to accelerate wound closure in mouse epidermis [23, 24]. Conversely, Cx43 has been shown to be upregulated in human chronic lower extremity ulcers and diabetic wounds, suggesting that downregulation is vital to normal wound healing and that dysregulation of this channel protein is involved in the

delayed closure observed in chronic wounds [25–27]. Understanding the mechanism of this dysreguation will lead to better understanding of how bacterial infections subvert the normal wound-healing scheme and give rise to new therapeutic targets for wound healing.

Considering the facts that Cx43 is involved in the migration of several types of cells [28–30] and *S. aureus* is found to impair wound closure [31], we investigated the relationship between the presence of *S. aureus* and Cx43 regulation in keratinocytes using both an in vitro cell migration model and an in vivo mouse cutaneous wound repair model. We also explored the possibility of manipulating wound closure of *S. aureus*-infected cutaneous wounds by interrupting the pathway for Cx43 production. Our work thus far sheds light on a mechanism for impaired wound closure observed in *S. aureus*-affected wounds and a candidate topical therapy that may improve the management of bacteria-affected wounds.

Materials and methods

Bacterial preparation

UAMS-1, a clinical *S. aureus* isolate, was grown on tryptic soy agar overnight. A single colony was selected and cultured in tryptic soy broth at 37 ℃ until the exponential growth phase was achieved. Bacteria were then centrifuged and resuspended in phosphate-buffered saline (PBS).

Exudate from in vitro grown *S. aureus* was prepared with a microfluidic platform based moderate-throughput in vitro BioFlux 200 system (Fluxion Biosciences, South San Francisco, CA) that is based on a microfluidic platform [32, 33]. This system allows the growth of bacteria in vitro mimicking host physiological conditions. Continuous culture medium perfusion was created in this system to support the growth of *S. aureus*. Meanwhile, the metabolic end products of *S. aureus* were removed at a low shear force. To enhance the attachment of *S. aureus* to the system, each flow channel of the BioFlux microplate was coated with 10 μg/ml human collagen type I (BD Bioscience, Bedford, MA) overnight at 4 ℃ prior to the inoculation of bacteria. The concentration of *S. aureus* inoculation was diluted to 0.1 of OD600. Fifty microliters of diluted *S. aureus* suspension was inoculated in the BioFlux 200 system. The inoculated *S. aureus* was allowed to grow in the system for 2 h. Thereafter, a brain heart infusion (BHI) medium supplemented with 1% glucose and 2% sodium chloride was applied to the system with a shear flow rate at 0.55 dyn/cm². The system was incubated at 37 ℃ overnight to create a *S. aureus* bacterial film in each channel. After the bacterial film was formed, 500 ml of medium flow-through was collected as exudate of in vitro *S. aureus* culture and filtered with 0.22 μm Bottle Top Vacuum Filter (Corning Inc., Corning, NY) to remove the bacteria

and debris. The collected medium was concentrated with 3 K MWCO Pierce™ Protein Concentrator (ThermoFisher Sci. Waltham, MA) and re-dissolved in 1 ml of PBS.

Keratinocyte migration assay

An immortalized human keratinocyte cell line, HaCaT, was used for the keratinocyte migration assay. HaCaT cells were cultured in Dulbecco's modified Eagle's medium (DMEM) medium-containing 10% fetal bovine serum (FBS) and 1% penicillin/streptomycin. HaCaT cells were seeded on 12-well culture plates at a density of 5×10^5 cells per well and allowed to reach 95% confluence. Cells were treated with 10 µg/ml of mitomycin C for 3 h followed by a wash with PBS.

To monitor keratinocyte migration, a fresh medium was added to each well and a single scratch was created with a micropipette tip across the center of the cell sheet. Photos were taken of the gap in each well under the microscope immediately after the creation of the scratch (time 0). Photos for each well were taken at five spots along the scratch and the spots were marked at the back of the plate. Medium in each well was then removed and PBS was added to wash the cell sheet and remove the floating cells. After the removal of PBS from each well, a fresh culture medium with 0.2% PBS (Control) or *S. aureus* exudate (SaE) was added in each well. The plate was incubated at 37 °C with 5% CO_2 for 16 h. Photos for the scratch in each well at the marked spots were taken again after 16-h incubation. The closure rate of each scratch on each cell sheet was calculated with the equation Gap closure rate $= (G0 - G16)/G0$, where G0 is the area of the gap in each photo at time 0 and G16 is the gap area at 16-h post-incubation. The area of each gap was measured with ImageJ [34].

To analyze the expression of Cx43 in migrating keratinocytes under the challenge of *S. aureus* exudate, we created scratch grids on each cell sheet. The width of each scratch was approximately 500 µm and the distance between two scratch marks was 500–1000 µm. Cells were treated with DMEM containing 0.2% PBS or *S. aureus* exudate for 1 or 2 days. Six replicates were harvested at each time point for RNA extraction. The relative expression levels of Cx43 in PBS- or SaE-treated cells at each time point were compared using quantitative PCR. Primers for Cx43 and internal reference (GAPDH) are listed in Table 1.

Cx43 knockdown in HaCaT cells using RNA interference (RNAi)

Functional analysis for Cx43 in keratinocytes was accomplished by RNAi. Short hairpin RNA (shRNA) was designed based on the mRNA sequence of human Cx43 (Table 2) and the validated shRNA sequence from the Millipore-Sigma

Table 1 qPCR primers used in this study.

Targeting gene	Sequence
GAPDH	Forward
	5′-TGTTGCCATCAATGACCCCTT-3′
	Reverse
	5′-CTCCACGACGTACTCAGCG-3′
Cx43	Forward
	5′-TCAAGCCTACTCAACTGCTGG-3′
	Reverse
	5′-TGTTACAACGAAAGGCAGACTG-3′

Table 2 Sequence information used for RNAi

Targeting gene	Sequence
Cx43	Forward: 5′-CCGGGCCCAAACTGATGGTGTCAATCTCGAGATTGACACCATCAGTTTGGGCTTTTTG-3′
	Reverse: 5′-AATTCAAAAAGCCCAAACTGATGGTGTCAATCTCGAGATTGACACCATCAGTTTGGGC-3′

MISSION® shRNA database (TRCN0000059773). Double-stranded shRNA was synthesized by Integrated DNA Technologies (IDT DNA, Coralville, IA) and cloned into pLKO.1 puro lentiviral vector (Addgene, Cambridge, MA). The production of lentivirus and transduction of lentiviral particles into host cells were performed according to the standard protocol specified by Addgene. The selection of transduced HaCaT cells was achieved by 2 µg/ml puromycin. The knockdown of Cx43 in HaCaT cells was confirmed by western blotting.

In vivo *S. aureus* infection in the mouse splinted excisional wound model

All the mice used in this study were housed at the Center for Comparative Medicine (CCM) at the Northwestern University, Feinberg School of Medicine. Procedures on experimental mice have been reviewed and approved by the Institutional Animal Care and Use Committee (IACUC). 8–10-week-old male C57BL/6 mice were obtained (Jackson Laboratory, Bar Harbor, ME) and housed in temperature and humidity controlled facility with a 12-h light–dark cycle, with food and water provided ad libitum. All experiments were conducted in accordance with the National Institutes of Health Guide for the care and use of laboratory animals.

Mice were anesthetized with inhaled isoflurane then shaved and depilated on the dorsum. A circular silicone splint with an 8-mm inner diameter was attached to the dorsal skin using n-butylcyanoacrylate adhesive and then sutured in place using interrupted 6-0 nylon suture. A sterile, disposable 6-mm punch biopsy instrument was utilized to mark the boundaries of the wound and iris scissors were utilized to excise a 6-mm diameter of skin down to the level of the panniculus carnosus. One wound was created on the dorsal area of each mouse. Each *S. aureus*-infected wound was inoculated with 10^7 colony-forming units (CFU) of *S. aureus*. Sterile control wounds were inoculated with the sterile PBS vehicle. Animals in the intervention group received a topical wound inoculation of LY294002 (Cell Signaling Technology, Danvers, MA) in DMSO solution, a PI 3 Kinase inhibitor, at the same time as bacterial inoculation (30 µg/wound). DMSO alone was used as the sham control. *S. aureus*-infected control animals received a topical wound inoculation with DMSO vehicle at the time of bacterial inoculation. The treatment and control were repeated every 2 days until the mice were harvested. Mouse bacterium-infected wound was created as previously described [35]. All wounds were covered with a semi-occlusive dressing (Tegaderm, 3 M, St. Paul, MN). Coban dressing was applied over the Tegaderm for protection from splint dislodgement. On the postoperative day (POD) 1, mupirocin ointment was applied to each wound to eradicate the non-adherent planktonic bacteria and the semi-occlusive dressing and Coban were replaced. On POD 3 an absorbent, non-adhesive dressing was applied to the wound bed to wick away exudate and Tegaderm and Coban were replaced. This dressing was replaced every other day until the day of the wound harvest.

Wounds were harvested on POD 7. After each animal was euthanized, full-thickness wounds were excised with a 4-mm diameter of unwounded tissue surrounding the wound bed. Each specimen was fixed in formalin phosphate 10% for at least 24 h. After appropriate fixation, the wounds were carefully bisected, paraffin-embedded, sectioned into 5 µm slices, and affixed to glass slides. For the measurements of epithelial gaps, granulation tissue areas, and newly generated epidermis during wound closure (neo-epidermis), slides were stained with hematoxylin and eosin and imaged using the Nikon Eclipse 50i bright-field microscope (Nikon Instruments, Melville, NY) and measured using ImageJ [36–38]. Five mice were used in each treatment and control group ($n = 5$).

Immunofluorescence (IF)

Immunofluorescence was used to detect the production of Cx43 in both keratinocytes and mouse skin. PBS- or SaE-treated HaCaT cells with a single scratch was washed with PBS and fixed in 4% paraformaldehyde at room temperature for 1 h. Following the removal of paraformaldehyde and three washes with PBS, cell samples were used for immunofluorescent staining using rabbit anti-human Cx43 polyclonal antibody (Sigma-Aldrich, St. Louis, MO) at 1:500 dilution in PBS following a standard IF protocol.

IF on animal tissues fixed by 10% formaldehyde was performed with the 5 µm sections. Briefly, the slides with paraffin-embedded tissue sections were first deparaffinized with 100% xylene followed by rehydration with serially diluted ethanol in PBS. Rehydrated sections were then incubated in antigen retrieval buffer (10 mM Sodium citrate, 0.05% Tween 20, pH 6.0) in a steamer for 20 min. Samples were then processed following the standard IF protocol. Cx43 antibody (Sigma-Aldrich) was diluted 1:500 with PBST (PBS containing 0.3% Triton X100), while the rabbit anti-human pAkt-S473 (Cell Signaling Technology) was diluted 1:200 with PBST. Secondary antibodies labeled with Alexa 488 or 594 (ThermoFisher Scientific) were applied with a 1:400 dilution for cell and tissue samples. Samples were observed under EVOS® FL Imaging System (ThermoFisher Scientific) and the images were taken with the integrated software.

Quantifications were done with the IF images of the HaCaT cell migration assay. Using the ImageJ software [34], the total Cx43 signal intensity of each image was measured and the total cell number in the same image was counted. The average Cx43 signal intensity in each cell was then calculated. The average Cx43 signal intensity in control group was used as the reference and the fold change of the average Cx43 signal intensity in *S. aureus* exudate-treated group was calculated and used to construct the bar graph.

Western blotting

Western blotting was used to check the efficiency of Cx43 knockdown in HaCaT cells. Whole-cell extracts were prepared using radioimmunoprecipitation assay buffer (50 mM Tris, 150 mM NaCl, 1% Triton X-100, 0.1% SDS, and 0.5% sodium deoxycholate, pH 7.5). Electrophoresis, transmembrane blotting, and antibody incubation were performed following standard protocols. Cx43 antibody was diluted 1:1000 with PBS containing 0.05% Tween20. Rabbit anti-human β-actin antibody (Sigma-Aldrich) was used as an internal reference with a 1:5000 dilution. Horseradish peroxidase-conjugated anti-rabbit immunoglobulin G (IgG) was used as a secondary antibody with a 1:5000 dilution. The signal of each band was translated into the total intensity by ImageJ. The values of signal intensities were used to show the difference in gene expression.

Protein kinase phosphorylation array with HaCaT cells

Human Phospho-Kinase Antibody Array kit (R&D Systems) was used to detect the keratinocyte protein kinase phosphorylation with the stimulation of *S. aureus* exudate. Wild-type HaCaT cells were seeded in an 8-well rectangular dish (ThermoFisher Scientific) and incubated with serum-free DMEM medium-containing 1% antibiotics at 37 ℃ for overnight. The scratch grids were created as described above following the treatment of 10 μg/ml of mitomycin C. SaE (0.2%) or PBS containing DMEM media was added as treatment and control respectively. HaCaT cells with both SaE treatment and control were harvested at 0, 30, 60, and 120 min post-treatment using cell lysis buffer provided by the kit. The procedures for protein kinase phosphorylation analysis were done according to the manufacturer's instruction. The developed film for each array membrane was scanned and analyzed using ImageJ. The signal intensity for each dot was digitalized by ImageJ and normalized with positive controls on each membrane. For each protein kinase, the relative phosphorylation level was calculated as the ratio of SaE treatment and control samples. A heat map of the overall relative phosphorylation levels of all kinases was constructed using Genesis [39]. The average values of each kinase were calculated with the four biological replicates of this experiment ($n = 4$).

Statistical analyses

For the comparisons in mRNA abundance (qPCR), the significance in difference was calculated by Student's *t* test analysis. For the multiple comparisons in cell migration rate (HaCaT migration assay) and wound closure (mouse splinted wound assay), one-way ANOVAs with post hoc Tukey's tests were used. The *p* values less than 0.05 were considered to be significantly different. The standard error of means (SEMs) were used in the figure to represent the error bars. The number of biological replicates (*n*) used in the analyses was described in the relevant figure legends.

Results

Cx43 expression is upregulated in migrating keratinocytes by *S. aureus* exudate

In vitro scratch assay showed that the migration of HaCaT covered $59.9 \pm 2.5\%$ of the gap that was created by the scratch after 16-h migration in the control condition. A significant delay of HaCaT migration was observed by 0.2% *S aureus* exudate treatment; $37.8 \pm 2.8\%$ closure (Fig. 1a). IF staining demonstrated a higher level of Cx43 production in the cells along the migrating edge of the scratch in the presence of *S. aureus* exudate compared to control (Fig. 1b). qPCR analysis showed upregulation of Cx43 in HaCaT by *S. aureus* exudate at day 1 and day 2 post-scratch, 3.0 ± 0.31- and 3.1 ± 0.51-fold, respectively (Fig. 1c). In addition, the relative Cx43 protein productions at day 1 post-treatment were estimated using the IF imaging analysis. The average Cx43 protein signal in *S. aureus*-treated HaCaT cells was 5.2 ± 2.09-fold higher than control HaCaT cells during gap closure (Fig. 1d).

Delayed migration of keratinocytes by *S. aureus* exudate is dependent on Cx43 expression in keratinocytes

We investigated whether Cx43 mediates the delay of keratinocyte migration in response to *S. aureus* exudate. We knocked down the expression of Cx43 in HaCaT cells with shRNA carried by lentivirus (Fig. 2a). Western blot analysis showed that the expression of Cx43 was reduced by 68% by shRNA mediated knockdown (Fig. 2a). The in vitro scratch assay showed that the migration of HaCaT cells was not affected by the Cx43 knockdown (Fig. 2b). Wild-type and Cx43 knockdown HaCaT cells showed that $56.3 \pm 2.7\%$ and $62.1 \pm 2.3\%$, respectively, of gap closure (Fig. 2c) at 16-h post-wounding. Treatment of *S. aureus* exudate in the culture medium inhibited the migration of wild-type HaCaT cells ($21.8 \pm 7.8\%$ gap closure). Interestingly, the migration of HaCaT was not inhibited by *S. aureus* exudate in Cx43knockdown HaCaT, $54.8 \pm 7.1\%$ gap closure (Fig. 2c). These data suggest that Cx43 is a key molecule mediating the delay of keratinocyte migration caused by *S. aureus* exudate.

Akt and ERK1/2 are involved in the response of keratinocytes to *S. aureus* exudate

Previous studies showed that the activation of Cx43 channels is mediated by kinase phosphorylation [40, 41]. Thus, we investigated protein kinase phosphorylation by *S. aureus* exudate (Fig. 3a). Among the 45 protein kinases tested in this study, Akt-S473 and ERK1/2 showed consistently upregulated phosphorylation levels by *S. aureus* exudate during HaCaT cell migration (Fig. 3b). Phosphorylation levels of Akt-S473 increased by 86.8, 78.3, and 133.7% after 30, 60, and 120 min *S. aureus* exudate treatment, respectively, compared to control (Fig. 3b). Phosphorylated ERK1/2 in *S. aureus* exudate-treated migrating HaCaT cells demonstrated 50.1, 60.2, and 64.5% increases at the three-time points, respectively, compared to controls (Fig. 3b). Other protein kinases, such as PRAS40, also showed a consistently upregulated phosphorylation profile with the treatment of *S.*
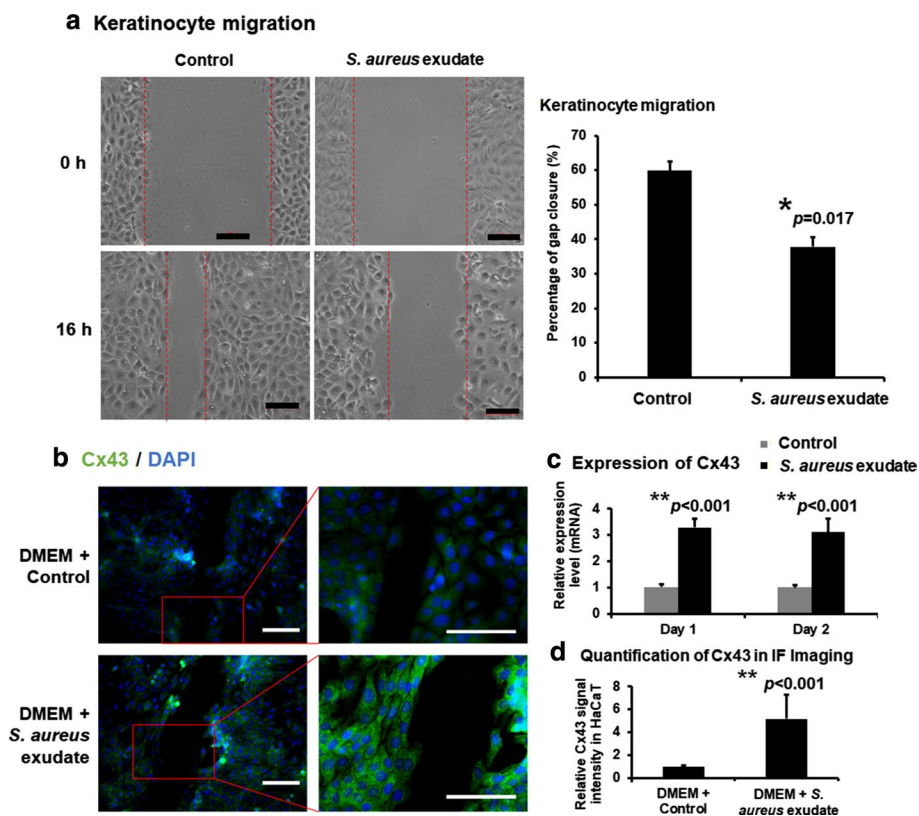
Fig. 1 *S. aureus* exudate upregulates Cx43 expression in migrating keratinocytes. **a**, **b** In vitro scratch assay. Closure rates were estimated at 16-h post-scratching and comparisons were made between control (PBS) and *S. aureus* exudate-treated HaCaT (*n* = 6) (**a**). Expression of Cx43 protein was estimated by immunofluorescent staining with the anti-Cx43 antibody at 16-h post-scratching (**b**). **c** Cx43 mRNA expression. Multiple scratches (grids) were made on HaCaT cul-ture, and control (PBS) or *S. aureus* exudate was treated. Cells were harvested at day 1 and 2 post-treatment and expression of Cx43 in *S. aureus* exudate-treated HaCaT was compared to control that is set as 1 (*n* = 6). **d** Cx43 protein expression. The expression of Cx43 protein in *S. aureus* exudate-treated HaCaT cells was compared to control HaCaT cells at day 1 by measuring the signal intensities of the IF images (*n* = 5). Scale bar: 100 μm. *$p < 0.05$, **$p < 0.01$

aureus exudate; however, it did not show a statistical difference from that in control.

## Inhibition of Akt phosphorylation enhances the closure of *S. aureus*-infected wound

A previously established splinted mouse skin excisional wound model [36] was adopted in this study (Fig. 4a). Wound healing was quantified by measuring epithelial migration on the H&E stained sections (Fig. 4b and Supplementary Fig. 1). Sterile wounds without *S. aureus* infection showed a 90.7 ± 3.2% closure at POD 7 (Fig. 4b, c). *S. aureus* infection significantly delayed the closure of the wound, 47.7 ± 2.0% closure at POD 7 (*p* < 0.001) (Fig. 4b, c). The topical treatment of PI3K/Akt inhibitor, 30 μg per wound, did not affect sterile wound closure, 95.0 ± 1.6% wound closure (Fig. 4b, c). In contrast, the application of PI3K/Akt inhibitor significantly accelerated the wound closure in *S. aureus*-infected wounds (74.7 ± 5.9% closure)

compared to the infected wounds without PI3K/Akt inhibitor (*p* = 0.007) (Fig. 4 b, c).

The area of granulation tissue was significantly increased in *S. aureus*-infected wound (1.76 ± 0.13 mm²) compared to the sterile wound (0.96 ± 0.12 mm², Fig. 4d). The application of PI3K/Akt inhibitor to the *S. aureus*-infected wound reduced the area of granulation tissue significantly (0.65 ± 0.16 mm², Fig. 4d). The length of new epidermis generated during wound closure (neo-epidermis) of the wound beds showed a similar pattern to the wound closure rate (Fig. 4e). The *S. aureus*-infected wounds showed the least neo-epidermis (1.08 ± 0.21 mm) among all treatment groups, while the lengths of neo-epidermis in sterile wounds without and with the treatment of PI3K/Akt inhibitor were 3.14 ± 0.57 mm and 3.12 ± 0.66 mm, respectively. The application of the PI3K/Akt inhibitor rescued the generation of neo-epidermis to 2.29 ± 0.27 mm.

The effects of PI3K/Akt inhibitor on keratinocyte migration was further tested in the in vitro scratch assay. Application of the PI3K/Akt inhibitor reversed the inhibition of

Fig. 2 Inhibition of keratinocyte migration by *S. aureus* exudate is not shown in Cx43 knockdown cells. **a** Cx43 knockdown in HaCaT. Whole-cell extract of wild type and Cx43 knockdown HaCaT were analyzed by Western blot analysis using Cx43 specific antibody. β-actin was used as a loading control. The intensities of the bands were quantified using ImageJ ($n = 4$). **b** In vitro migration scratch assay. Migrations of wild-type and Cx43 knockdown HaCaT cells was compared in the presence (or absence) of *S. aureus* exudate. **c** Quantification of migration. The differences in cell migration were calculated using one-way ANOVA with Tukey's test for multiple comparisons ($n = 6$). WT: wild type; KD: knockdown; SaE: *S. aureus* exudate. Scale bar: 100 μm. $*p < 0.05$, $**p < 0.01$
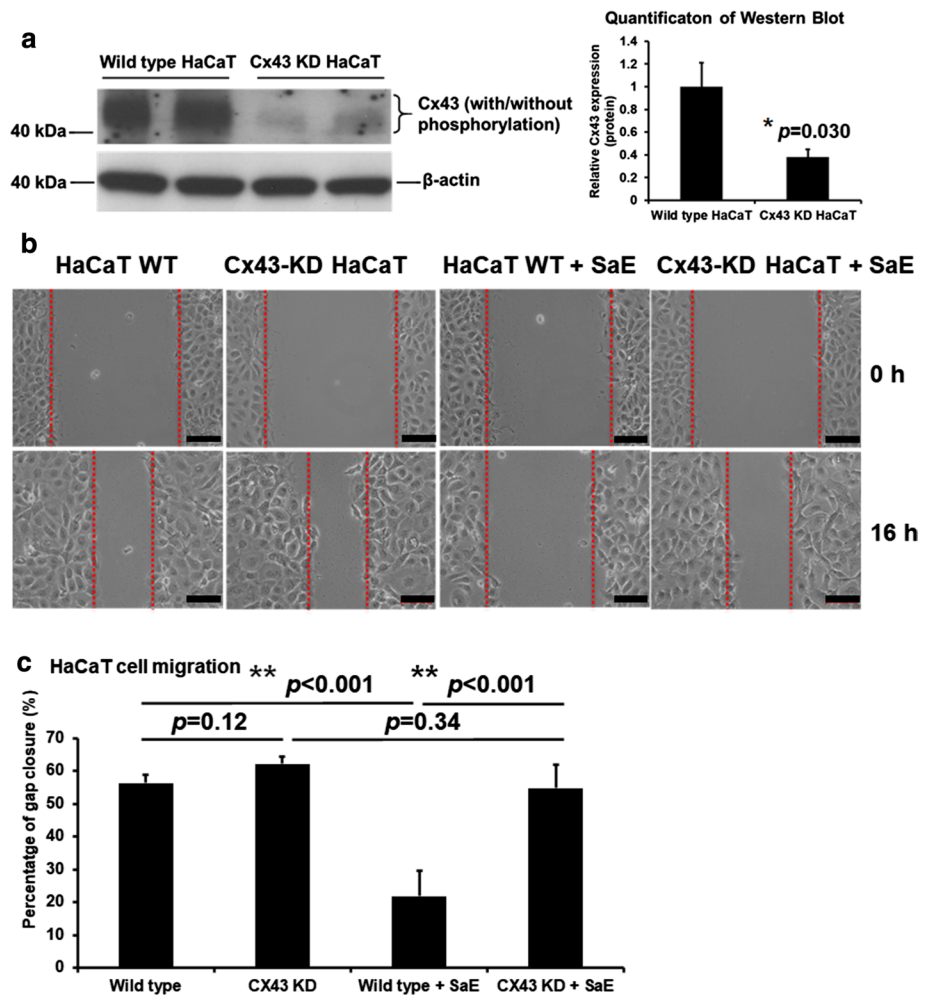
HaCaT cell migration, which was caused by *S. aureus* exudate, from 18.9 ± 3.2 to $60.2 \pm 1.8\%$ (Supplementary Fig. 2).
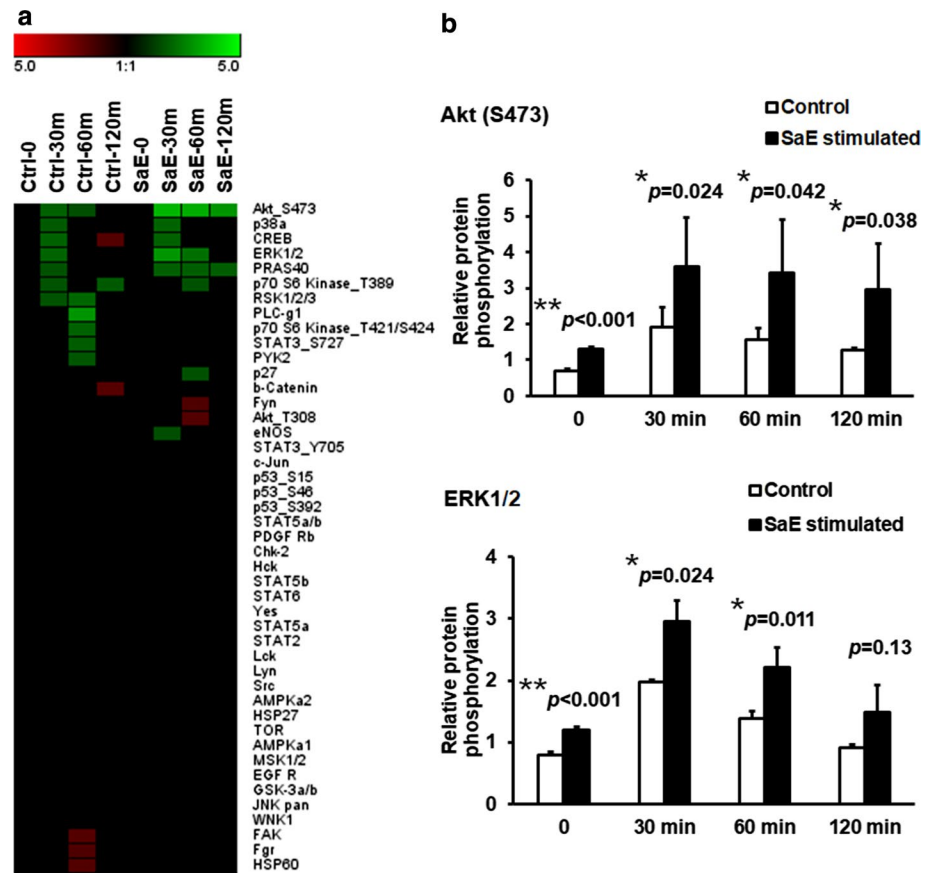
Administration of PI3K/Akt inhibitor in *S. aureus*-infected mouse wound inhibited not only the phosphorylation of Akt-S473 but also the expression of Cx43 in the wounding area

In normal conditions, the sterile mouse excisional skin wound showed a low level of Akt-S473 phosphorylation in the epidermis of wound edges (Fig. 5a, labeled as sterile, which was treated with DMSO only). The phosphorylation level of Akt-S473 in the epidermis of the wound bed was significantly elevated with an infection of *S. aureus* (Fig. 5a, labeled as *S. aureus*, which was treated with *S. aureus* and DMSO). A $94.2 \pm 7.7\%$ of increase of pAkt signal intensity was found in *S. aureus*-infected wounds compared to the sterile wounds (Fig. 5c). Repeated topical administration of the PI3K/Akt inhibitor in the wounding area significantly decreased the phosphorylation level of Akt-S473 in the migration epithelial edge of *S. aureus*-infected wounds (Fig. 5a, labeled as S. aureus + PI3K/Akt inhibitor, which was treated with *S. aureus* and PI3K/Akt inhibitor in DMSO). Quantification showed that a reduction of phosphorylated Akt by the PI3K/Akt inhibitor treatment in *S. aureus*-infected wounds; $42.4 \pm 6.8\%$ of *S. aureus*-infected wounds (Fig. 5c).

Next, we analyzed the expression level of Cx43 that is downstream of Akt. The upregulation of Cx43 production was observed in the epidermis of *S. aureus*-infected wounds compared to sterile ones; 1.94 ± 0.24-fold increase (Fig. 5b, d). Inhibition of Akt-S473 phosphorylation by the PI3K/Akt inhibitor in the *S. aureus*-infected mouse wound bed also downregulated the expression of Cx43, which results in a level of $95.0 \pm 5.5\%$ in the sterile wounds (Fig. 5b, d). A control experiment showed that the application of the PI3K/Akt inhibitor marginally decreased production of Akt phosphorylation (Fig. 5a, c) or Cx43 expression (Fig. 5b, d) in the sterile wounds, which is statistically insignificant. Overlay of the IF images showed that most epidermal cells expressed both Cx43 and pAkt (Supplementary Fig. 3).

Fig. 3 Phosphorylated Akt and ERK1/2 were upregulated by *S. aureus* exudate. Protein kinase phosphorylation array. The whole-cell extract was prepared from in vitro scratched HaCaT that was grown in the presence of *S. aureus* exudate for 0, 30, 60, and 120 min. Phosphorylation of protein kinases was analyzed using a protein array that contains 45 protein kinases. The level of phosphorylation was compared to control, HaCaT grown in the absence of *S. aureus* exudate. **a** Heat map. Green and red represent upregulation and downregulation, respectively, compared to control ($n=4$). **b** Quantification of phosphorylation of Akt-S473 and ERK1/2. SaE: *S. aureus* exudate. $n=4$ *$p<0.05$, **$p<0.01$

Discussion

Among the over 20 members of the connexin protein family, many of them in recent years have been shown to be involved in the control of cell migration. It has been shown in vitro that several connexins play critical roles in cell migration in a variety of cells, such as brain-derived cells [42, 43], fibroblast cells [44, 45], endothelial and endothelial progenitor cells [46, 47], epithelioid cells [46], and cardiac cells [48]. In vivo studies showed a high expression of Cx43 present in migrating neural crest cells which are involved in brain and heart development [49, 50]. Moreover, Cx43 was also found to be highly expressed in migrating endothelial cells during wound closure [51, 52]. We are, therefore,

We further verified the in vivo results in vitro cultured HaCaT cells. Application of PI3K/Akt inhibitor did not change the expression levels of Cx43 at the migrating edge of the sterile HaCaT cell culture (Supplementary Fig. 4 a, b, e). Treatment of *S. aureus* exudate increased the expression of Cx43 by 5.2 ± 2.1-fold compared to sterile control. PI3K/Akt inhibitor treatment lowered the Cx43 expression in *S. aureus* exudate-treated HaCaT (Supplementary Fig. 4c–e).

particularly interested in studying the roles of Cx43 in regulating keratinocyte migration during wound repair.

The upregulation of Cx43 expression in keratinocytes was observed when the cells were treated with *S. aureus* exudate that inhibited the collective migration of keratinocytes. However, it is noteworthy that inhibition of Cx43 production did not significantly enhance the keratinocyte migration in the normal condition (Fig. 2). Previous studies demonstrated that the downregulation of Cx43 in keratinocytes at the skin margins was observed during normal wound healing [20–22]. This probably can be used to explain why knockdown of Cx43 in keratinocytes did not affect much in collective cell migration. In contrast, when keratinocyte migration was significantly delayed by *S. aureus* exudate, the expression level of Cx43 at the edges of migrating cells was upregulated. Therefore, inhibition of Cx43 expression results in the delay of migration only in *S. aureus*-infected keratinocytes but not wild-type keratinocytes.

Phosphorylation array performed on the HaCaT cells in our in vitro experiments showed a marked increase in Akt phosphorylation in cells from the scratch-wound margins exposed to *S. aureus* exudate compared to controls. Akt (also known as Protein kinase B, PKB) is a serine/threonine-protein kinase known to regulate a variety of cellular processes including growth, metabolism, survival, proliferation, and
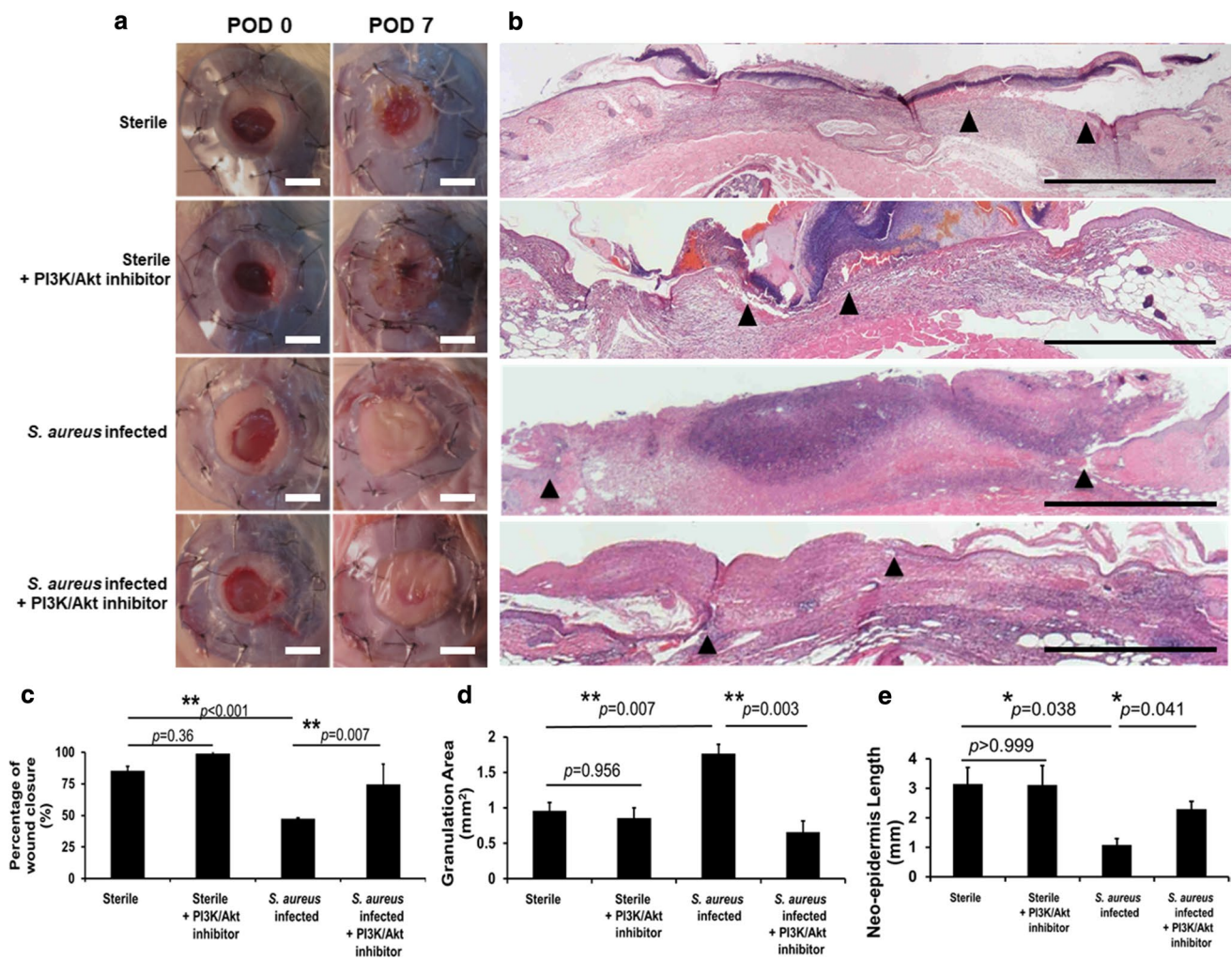
Fig. 4 Inhibition of PI3K/Akt enhances wound healing of *S. aureus*-infected wound. Sterile or *S. aureus*-infected wounds were treated with 30 µg/wound of PI3K/Akt inhibitor (LY294002). **a** Photograph of wounds at day 7. Scale bar: 3 mm. **b** Histological analysis of wounds. H&E staining was performed on sectioned wound samples. Migrating epithelial edges of the wound were indicated by arrowheads. Scale bar: 1 mm. **c** Measurement of the wound healing rate. The distance of the epithelial gap in each wound was measured and presented as the percentage of wound closure. **d** Quantification of graluation tissues. **e** Quantification the total length of the newly generated epidermis during wound closure (neo-epidermis). All measurements were done with ImageJ. The differences in wound closure rates, granulation tissue areas, and neo-epidermis length were calculated using one-way ANOVA with Tukey's test for multiple comparisons ($n=5$), $*p<0.05$, $**p<0.01$

angiogenesis. Akt has been shown to phosphorylate Cx43 on serine-369 and serine-373 residues and has been implicated as a prime regulator of Cx43 activity and gap junction stability [53, 54]. The previous findings suggested that Akt-mediated phosphorylation of Cx43 exerted greater control over gap junctional stability and turnover than the ubiquitination of the protein itself [54]. Replacement of the protein's ubiquitination sites did not affect the localization of gap junctional size. However, Akt phosphorylation enhanced stability via regulating the size of gap junctions. The blockade of Akt activation resulted in a greater turnover of gap junctions and reduced gap junctional size [54]. In vivo, there was also more robust immunofluorescent staining for phosphorylated

Akt in *S. aureus*-infected wounds compared to controls. The blockade of Akt phosphorylation also diminished the signal of Cx43 in the wound bed epidermis. This indicated that the function of Cx43 may be disrupted by interrupting the PI3K/Akt pathway.

We applied the Akt inhibitor to disrupt the function of Cx43 and accelerate epithelial keratinocyte migration that is impaired by *S. aureus* infection. As we expected, the *S. aureus* exudate-treated HaCaT cells with Akt inhibitor lead to statistically significant improvement in keratinocyte migration compared to the *S. aureus* exudate cells without Akt inhibitor treatment (Supplementary Fig. 2). Additionally, we applied topical Akt inhibitor to our *S.*

Fig. 5 Increased expression of p-AKT and Cx43 by *S. aureus* exudate is lowered by PI3K/Akt inhibition. *S. aureus*-infected wounds were treated with 10 µg of LY294002. **a**, **b** Expression of phosphorylated Akt (**a**) and Cx43 (**b**) was analyzed in sterile, LY294002-treated, *S. aureus*-infected, and LY294002-treated *S. aureus*-infected wounds with their specific antibodies. The signal was visualized with a fluorescence-labeled secondary antibody. The migrating epithelial edge of each wound was indicated by an arrowhead. The basal layer of the epidermis was indicated by dashed white lines. (**c**, **d**) The immunofluorescent images of phosphorylate Akt (**c**) and Cx43 (**d**) were quantified by ImageJ ($n = 5$). SaE: *S. aureus* exudate. $**p < 0.01$. Scale bar: 100 µm
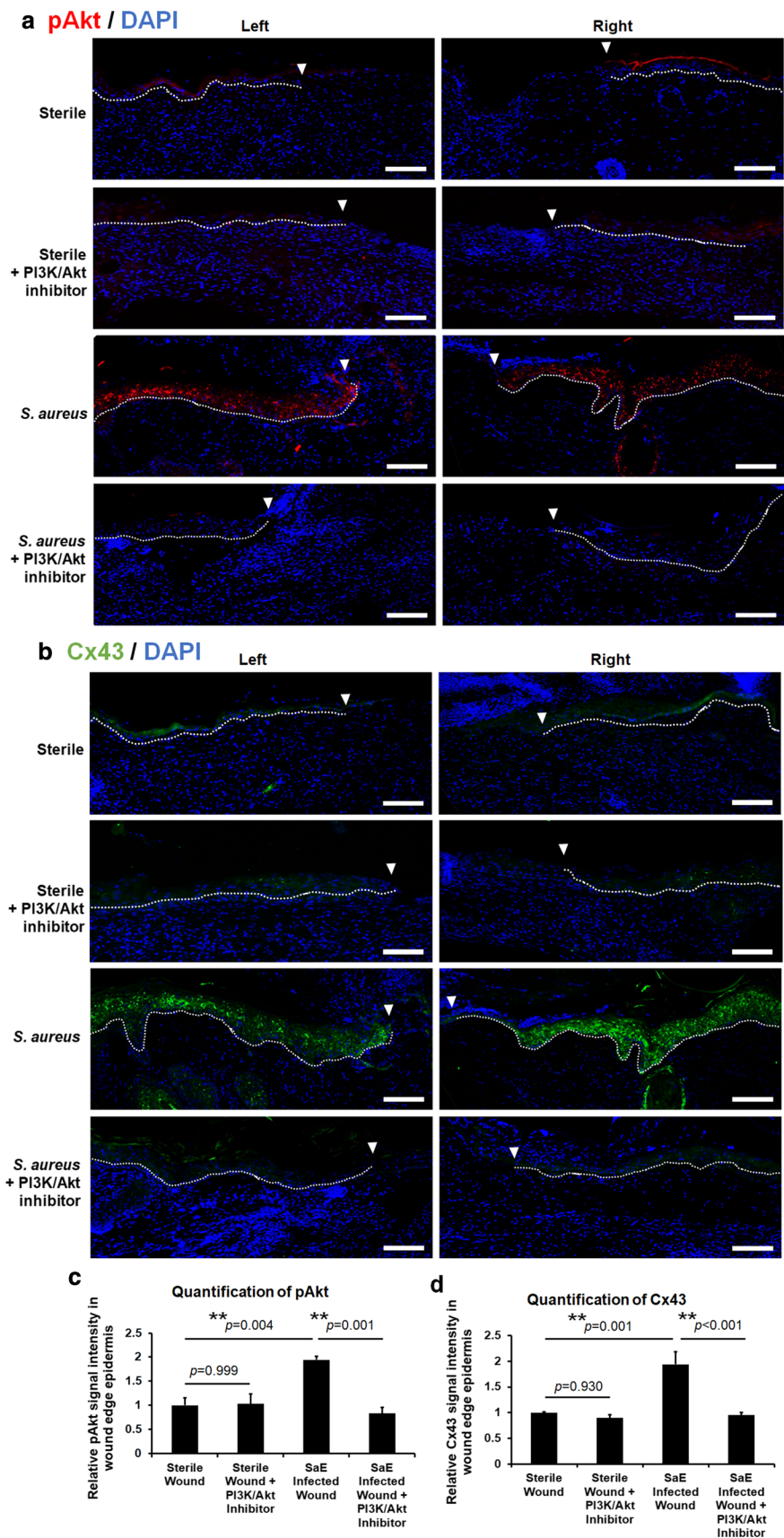
aureus-infected splinted dorsal wounds in C57BL/6 mice and found improved re-epithelialization and wound closure compared to those exposed to *S. aureus* only.

The Akt inhibitor used in our study, LY294002, is a commonly used pharmacologic inhibitor that selectively inhibits the phosphoinositide 3-kinase-Akt nexus. It has been used in many PI3K/Akt pathway-related studies. For example, LY294002 inhibited the growth, migration, and invasion of human osteosarcoma cells [55]. This inhibitor also demonstrated the capability of altering the expression of IL-10 and TNF-α in macrophages [56]. Our study showed that the application of LY294022 on *S. aureus*-infected mouse cutaneous wounds significantly reduced the number of Cx43 in the epidermis of the wound area. It also dramatically enhanced the wound closure of the *S. aureus*-infected wounds. However, the effects of the inhibitor on the stromal cells in the dermis, such as fibroblast cells, endothelial cells, and macrophages, were not investigated in the present study. Given that the PI3K/Akt pathway is employed by many cell types [57], it is likely that the application of the PI3K/Akt inhibitor will also interfere with the cellular process of other types of cells in the wound bed. Another study demonstrated the inhibition of wound closure by a PI3K/Akt inhibitor in rat sterile wounds through the prevention of fibroblast cell contraction in wounding areas [58]. In our study, the effects of the PI3K/Akt inhibitor on wound repair were not observed in sterile wounds. However, it improved the wound closure in *S. aureus*-infected wounds, which suggested that this method may only benefit the cutaneous wounds with increased inflammatory conditions. It can, therefore, be potentially used as a new therapeutic strategy for the treatment of bacteria-infected human wounds.

References

1. Nussbaum SR, Carter MJ, Fife CE, DaVanzo J, Haught R, Nusgart M, Cartwright D (2018) An Economic evaluation of the impact, cost, and medicare policy implications of chronic nonhealing wounds. Value Health 21(1):27–32. https://doi.org/10.1016/j.jval.2017.07.007

2. James GA, Swogger E, Wolcott R, Pulcini E, Secor P, Sestrich J, Costerton JW, Stewart PS (2008) Biofilms in chronic wounds. Wound Repair Regen 16(1):37–44. https://doi.org/10.1111/j.1524-475X.2007.00321.x

3. Siddiqui AR, Bernstein JM (2010) Chronic wound infection: facts and controversies. Clin Dermatol 28(5):519–526. https://doi.org/10.1016/j.clindermatol.2010.03.009

4. Edwards R, Harding KG (2004) Bacteria and wound healing. Curr Opin Infect Dis 17(2):91–96

5. Malone M, Bjarnsholt T, McBain AJ, James GA, Stoodley P, Leaper D, Tachi M, Schultz G, Swanson T, Wolcott RD (2017) The prevalence of biofilms in chronic wounds: a systematic review and meta-analysis of published data. J Wound Care 26(1):20–25. https://doi.org/10.12968/jowc.2017.26.1.20

6. Bowler PG, Duerden BI, Armstrong DG (2001) Wound microbiology and associated approaches to wound management. Clin Microbiol Rev 14(2):244–269. https://doi.org/10.1128/CMR.14.2.244-269.2001

7. Gardner SE, Frantz RA, Doebbeling BN (2001) The validity of the clinical signs and symptoms used to identify localized chronic wound infection. Wound Repair Regen 9(3):178–186

8. Brook I, Frazier EH (1998) Aerobic and anaerobic microbiology of chronic venous ulcers. Int J Dermatol 37(6):426–428

9. Power C, Wang JH, Sookhai S, Street JT, Redmond HP (2001) Bacterial wall products induce downregulation of vascular endothelial growth factor receptors on endothelial cells via a CD14-dependent mechanism: implications for surgical wound healing. J Surg Res 101(2):138–145. https://doi.org/10.1006/jsre.2001.6270

10. Konturek PC, Brzozowski T, Konturek SJ, Kwiecien S, Dembinski A, Hahn EG (2001) Influence of bacterial lipopolysaccharide on healing of chronic experimental ulcer in rat. Scand J Gastroenterol 36(12):1239–1247

11. Becker DL, Thrasivoulou C (1818) Phillips AR (2012) Connexins in wound healing; perspectives in diabetic patients. Biochim Biophys Acta 8:2068–2075. https://doi.org/10.1016/j.bbamem.2011.11.017

12. Malminen M, Koivukangas V, Peltonen J, Karvonen SL, Oikarinen A, Peltonen S (2003) Immunohistological distribution of the tight junction components ZO-1 and occludin in regenerating human epidermis. Br J Dermatol 149(2):255–260

13. Chavez MG, Buhr CA, Petrie WK, Wandinger-Ness A, Kusewitt DF, Hudson LG (2012) Differential downregulation of e-cadherin and desmoglein by epidermal growth factor. Dermatol Res Pract 2012:309587. https://doi.org/10.1155/2012/309587

14. Safferling K, Sutterlin T, Westphal K, Ernst C, Breuhahn K, James M, Jager D, Halama N, Grabe N (2013) Wound healing revised: a novel reepithelialization mechanism revealed by in vitro and in silico models. J Cell Biol 203(4):691–709. https://doi.org/10.1083/jcb.201212020

15. Hodgins MB (2004) Connecting wounds with connexins. J Invest Dermatol 122(5):9–10. https://doi.org/10.1111/j.0022-202X.2004.22535.x

16. Richard G (2000) Connexins: a connection with the skin. Exp Dermatol 9(2):77–96

17. Richard G (2005) Connexin disorders of the skin. Clin Dermatol 23(1):23–32. https://doi.org/10.1016/j.clindermatol.2004.09.010

18. Common JE, Becker D, Di WL, Leigh IM, O'Toole EA, Kelsell DP (2002) Functional studies of human skin disease- and deafness-associated connexin 30 mutations. Biochem Biophys Res Commun 298(5):651–656

19. van Steensel MA (2004) Gap junction diseases of the skin. Am J Med Genet C Semin Med Genet 131C(1):12–19. https://doi.org/10.1002/ajmg.c.30030

20. Chanson M, Derouette JP, Roth I, Foglia B, Scerri I, Dudez T, Kwak BR (2005) Gap junctional communication in tissue inflammation and repair. Biochim Biophys Acta 1711(2):197–207. https://doi.org/10.1016/j.bbamem.2004.10.005

21. Goliger JA, Paul DL (1995) Wounding alters epidermal connexin expression and gap junction-mediated intercellular communication. Mol Biol Cell 6(11):1491–1501

22. Coutinho P, Qiu C, Frank S, Tamber K, Becker D (2003) Dynamic changes in connexin expression correlate with key events in the wound healing process. Cell Biol Int 27(7):525–541

23. Qiu C, Coutinho P, Frank S, Franke S, Law LY, Martin P, Green CR, Becker DL (2003) Targeting connexin43 expression accelerates the rate of wound repair. Curr Biol 13(19):1697–1703

24. Kretz M, Euwens C, Hombach S, Eckardt D, Teubner B, Traub O, Willecke K, Ott T (2003) Altered connexin expression and wound healing in the epidermis of connexin-deficient mice. J Cell Sci 116(Pt 16):3443–3452. https://doi.org/10.1242/jcs.00638

25. Brandner JM, Houdek P, Husing B, Kaiser C, Moll I (2004) Connexins 26, 30, and 43: differences among spontaneous, chronic, and accelerated human wound healing. J Invest Dermatol 122(5):1310–1320. https://doi.org/10.1111/j.0022-202X.2004.22529.x

26. Bajpai S, Shukla VK, Tripathi K, Srikrishna S, Singh RK (2009) Targeting connexin 43 in diabetic wound healing: future perspectives. J Postgrad Med 55(2):143–149. https://doi.org/10.4103/0022-3859.48786

27. Wang CM, Lincoln J, Cook JE, Becker DL (2007) Abnormal connexin expression underlies delayed wound healing in diabetic skin. Diabetes 56(11):2809–2817. https://doi.org/10.2337/db07-0613

28. Kameritsch P, Pogoda K (1818) Pohl U (2012) Channel-independent influence of connexin 43 on cell migration. Biochim Biophys Acta 8:1993–2001. https://doi.org/10.1016/j.bbamem.2011.11.016

29. Wright CS, van Steensel MA, Hodgins MB, Martin PE (2009) Connexin mimetic peptides improve cell migration rates of human epidermal keratinocytes and dermal fibroblasts in vitro. Wound Repair Regen 17(2):240–249. https://doi.org/10.1111/j.1524-475X.2009.00471.x

30. Ghosh S, Kumar A, Tripathi RP, Chandna S (2014) Connexin-43 regulates p38-mediated cell migration and invasion induced selectively in tumour cells by low doses of gamma-radiation in an ERK-1/2-independent manner. Carcinogenesis 35(2):383–395. https://doi.org/10.1093/carcin/bgt303

31. Schierle CF, De la Garza M, Mustoe TA, Galiano RD (2009) Staphylococcal biofilms impair wound healing by delaying reepithelialization in a murine cutaneous wound model. Wound Repair Regen 17(3):354–359. https://doi.org/10.1111/j.1524-475X.2009.00489.x

32. Chen P, Abercrombie JJ, Jeffrey NR, Leung KP (2012) An improved medium for growing Staphylococcus aureus biofilm. J Microbiol Methods 90(2):115–118. https://doi.org/10.1016/j.mimet.2012.04.009

33. Chen P, Seth AK, Abercrombie JJ, Mustoe TA, Leung KP (2014) Activity of imipenem against Klebsiella pneumoniae biofilms in vitro and in vivo. Antimicrob Agents Chemother 58(2):1208–1213. https://doi.org/10.1128/AAC.01353-13

34. Schneider CA, Rasband WS, Eliceiri KW (2012) NIH Image to ImageJ: 25 years of image analysis. Nat Methods 9(7):671–675

35. Nguyen KT, Seth AK, Hong SJ, Geringer MR, Xie P, Leung KP, Mustoe TA, Galiano RD (2013) Deficient cytokine expression and neutrophil oxidative burst contribute to impaired cutaneous wound healing in diabetic, biofilm-containing chronic wounds. Wound Repair Regen 21(6):833–841. https://doi.org/10.1111/wrr.12109

36. Galiano RD, Jt M, Dobryansky M, Levine JP, Gurtner GC (2004) Quantitative and reproducible murine model of excisional wound healing. Wound Repair Regen 12(4):485–492. https://doi.org/10.1111/j.1067-1927.2004.12404.x

37. Haertel E, Joshi N, Hiebert P, Kopf M, Werner S (2018) Regulatory T cells are required for normal and activin-promoted wound repair in mice. Eur J Immunol 48(6):1001–1013. https://doi.org/10.1002/eji.201747395

38. Chen L, Mirza R, Kwon Y, DiPietro LA, Koh TJ (2015) The murine excisional wound model: contraction revisited. Wound Repair Regen 23(6):874–877. https://doi.org/10.1111/wrr.12338

39. Sturn A, Quackenbush J, Trajanoski Z (2002) Genesis: cluster analysis of microarray data. Bioinformatics 18(1):207–208

40. Batra N, Riquelme MA, Burra S, Kar R, Gu S, Jiang JX (2014) Direct regulation of osteocytic connexin 43 hemichannels through AKT kinase activated by mechanical stimulation. J Biol Chem 289(15):10582–10591. https://doi.org/10.1074/jbc.M114.550608

41. Solan JL, Lampe PD (2009) Connexin43 phosphorylation: structural changes and biological effects. Biochem J 419(2):261–272. https://doi.org/10.1042/BJ20082319

42. Bates DC, Sin WC, Aftab Q, Naus CC (2007) Connexin43 enhances glioma invasion by a mechanism involving the carboxy terminus. Glia 55(15):1554–1564. https://doi.org/10.1002/glia.20569

43. Homkajorn B, Sims NR, Muyderman H (2010) Connexin 43 regulates astrocytic migration and proliferation in response to injury. Neurosci Lett 486(3):197–201. https://doi.org/10.1016/j.neulet.2010.09.051

44. Wei CJ, Francis R, Xu X, Lo CW (2005) Connexin43 associated with an N-cadherin-containing multiprotein complex is required for gap junction formation in NIH3T3 cells. J Biol Chem 280(20):19925–19936. https://doi.org/10.1074/jbc.M412921200

45. Moorby CD (2000) A connexin 43 mutant lacking the carboxyl cytoplasmic domain inhibits both growth and motility of mouse 3T3 fibroblasts. Mol Carcinog 28(1):23–30

46. Behrens J, Kameritsch P, Wallner S, Pohl U, Pogoda K (2010) The carboxyl tail of Cx43 augments p38 mediated cell migration in a gap junction-independent manner. Eur J Cell Biol 89(11):828–838. https://doi.org/10.1016/j.ejcb.2010.06.003

47. Pepper MS, Montesano R, el Aoumari A, Gros D, Orci L, Meda P (1992) Coupling and connexin 43 expression in microvascular and large vessel endothelial cells. Am J Physiol 262(5 Pt 1):C1246–1257

48. Liu X, Liu W, Yang L, Xia B, Li J, Zuo J, Li X (2007) Increased connexin 43 expression improves the migratory and proliferative ability of H9c2 cells by Wnt-3a overexpression. Acta Biochim Biophys Sin (Shanghai) 39(6):391–398

49. Huang GY, Cooper ES, Waldo K, Kirby ML, Gilula NB, Lo CW (1998) Gap junction-mediated cell-cell communication modulates mouse neural crest migration. J Cell Biol 143(6):1725–1734

50. Lo CW, Waldo KL, Kirby ML (1999) Gap junction communication and the modulation of cardiac neural crest cells. Trends Cardiovasc Med 9(3–4):63–69

51. Pepper MS, Spray DC, Chanson M, Montesano R, Orci L, Meda P (1989) Junctional communication is induced in migrating capillary endothelial cells. J Cell Biol 109(6 Pt 1):3027–3038

52. Pepper MS, Meda P (1992) Basic fibroblast growth factor increases junctional communication and connexin 43 expression in microvascular endothelial cells. J Cell Physiol 153(1):196–205. https://doi.org/10.1002/jcp.1041530124

53. Park DJ, Wallick CJ, Martyn KD, Lau AF, Jin C, Warn-Cramer BJ (2007) Akt phosphorylates connexin 43 on Ser373, a "mode-1" binding site for 14–3-3. Cell Commun Adhes 14(5):211–226. https://doi.org/10.1080/15419060701755958

54. Dunn CA, Su V, Lau AF, Lampe PD (2012) Activation of Akt, not connexin 43 protein ubiquitination, regulates gap junction stability. J Biol Chem 287(4):2600–2607. https://doi.org/10.1074/jbc.M111.276261

55. Long XH, Zhong ZH, Peng AF, Zhu LB, Wang H, Zhang GM, Liu ZL (2014) LY294002 suppresses the malignant phenotype and sensitizes osteosarcoma cells to pirarubicin chemotherapy. Mol Med Rep 10(6):2967–2972. https://doi.org/10.3892/mmr.2014.2617

56. Avni D, Glucksam Y, Zor T (2012) The phosphatidylinositol 3-kinase (PI3K) inhibitor LY294002 modulates cytokine expression in macrophages via p50 nuclear factor kappaB inhibition, in a PI3K-independent mechanism. Biochem Pharmacol 83(1):106–114. https://doi.org/10.1016/j.bcp.2011.09.025

57. Hemmings BA, Restuccia DF (2015) The PI3K-PKB/Akt Pathway. Csh Perspect Biol 7(4):a011189

58. Li G, Li YY, Sun JE, Lin WH, Zhou RX (2016) ILK-PI3K/ AKT pathway participates in cutaneous wound contraction by regulating fibroblast migration and differentiation to myofibroblast. Lab Invest 96(7):741–751. https://doi.org/10.1038/labinvest.2016.48